shielding factors.

We may extend this relation to a lower $\Delta A > 2$, modifying ΔA by +4 to $\Delta A'$, and minor changes to shielding factors [1], $P(^{38}Ar)_{metal} = f \times k_1' \times 22^{-k2'}$.

Even for small mass products, such as He and ^{10}Be, the above formulations are applicable. Normalized production functions for He isotopes can be compared with those of A = 38 and 46 [2], $P(^3He)_{metal} = 16.7 \times k_1' \times 22^{-k2'}$; $P(^4He)_{metal} = 18.3 \times k_1' \times 14^{-k2'}$. Eliminating shielding factors, two ratios of three to four species are plotted in power functions having a slope in terms of $\Delta A'$, $d \log(P_1/P_2)/d \log (P_3/P_4) = \log(\Delta A_1'/\Delta A_2')/\log(\Delta A_3'/\Delta A_4')$.

"Multielement Target": The behavior of He can be attributed to the variable cross sections in an extended range. The excitation function is equivalent to that of a mixture of several species of products induced at different threshold energies [3], requiring a model of multielement targets for a certain product. A typical constantly mixed target is a chondrite.

In 1979 Voshage and Feldman demonstrated $(^3He/^{38}Ar)_{metal}$ are almost constant, but slightly higher under extreme shielding, which is common with those targets.

Recent results with a set of Brenham pallasite are given from the extremely wide shielding and the practical absence of radiogenic products [4].

Helium in Stone: In chondrites, most ^4He is from natural radioactivities. In Brenham, the largest meteoritic stone, cosmogenic ^4He is predominant even in the heaviest shielded samples. Helium-3/helium-4 in stone and metal is plotted parallel against $(^4He/^{21}Ne)_{metal}$. Cosmogenic He in stone can be formulated just as in metal with the following relations applied as second-order approximations

$$P(^3He)_{st}/(23 \times k_{1'} \times 22^{-k2'}) = 1 + 0.3 \times (k_{2'} - 2.3)^2$$

$$P(^4He)_{st}/(36 \times k_{1'} \times 13^{-k2'}) = 1 + 0.2 \times (k_{2'} - 2.4)^2$$

Argon Isotopes: A plot for Ar isotopes is made for Brenham, and radiogenic Ar estimated from the three-isotope plot. Based on the data, two sets of plots, metal and stone, can be superimposed. The contributions from Ca and Cl seem neglible due to lower contents. In the metal phase, radiogenic Ar is insignificant, and the olivine seems to contain the lowest ^{40}Ar equivalent, <0.01 ppm K. Direct determinations for K in Brenham olivine have been performed by radiochemical neutron activation, with figures as low as 0.01 ppm K observed [5].

Beryllium-10 in Metal: Beryllium-10 and ^{36}Cl are compared because their ratios are indicators for terrestrial age. The ratio in fresh meteorites is about 5. A ratio of around 4 was found in the smallest objects, and 5.5–6 was observed in heavily shielded Brenham [6]. Older parameters, $\Delta A' = 22$ and $f = 0.11$, for $^{10}Be_{metal}$ are revised to $\Delta A' = 28$ and $f = 0.18$.

References: [1] Imamura M. et al. (1980) *Z. Naturforsch., 35a*, 267–279. [2] Honda M. (1985) *EPSL, 75*, 77–80. [3] Honda M. (1988) *Meteoritics, 23*, 3–13. [4] Honda M. et al. (1996) *Meteoritics & Planet. Sci., 31*, A98–A99; personal communication.

THE FORMATION OF CARBONYL SULFIDE (OCS) IN VENUS' LOWER ATMOSPHERE.

Y. Hong and B. Fegley Jr., Planetary Chemistry Laboratory, Department of Earth and Planetary Sciences, Washington University, St. Louis MO 63130-4899, USA (yhong@levee.wustl.edu; bfegley@levee.wustl.edu).

Introduction: Carbonyl sulfide (OCS) is the dominant reduced-S gas and is the second most abundant S gas, after SO_2, observed below Venus' clouds [1,2]. The chemical reactions involved in the formation and decomposition of OCS are important for the oxidation state of Venus' lower atmosphere, for geochemistry of the surface, and for the maintenance of the global H_2SO_4 acid clouds. According to the Venus S cycle [3-5], there are three possible sources of OCS:

$$2\ CO + S_2 = 2\ OCS \quad (1)$$

$$3\ FeS_2 + 4\ CO_2 + 2\ CO = Fe_3O_4 + 6\ OCS \quad (2)$$

$$SO_2 + 3\ CO = OCS + 2\ CO_2 \quad (3)$$

TABLE 1. OCS concentrations in CO-CO_2 gas mixtures.

Temperature (Celsius)	ppmv OCS 0.2% CO	ppmv OCS 0.5% CO	OCS ratio 0.5%/0.2%
471	19.0	49.3	2.59
498	60.4	157	2.60
524	211	504	2.39
551	574	1,290	2.25
580	899	2,260	2.51
		Observed:	2.47 ± 0.15
		Predicted:	2.50

However, no data on the rates of OCS formation and decomposition are currently available. In this work we present a kinetic study of OCS formation reactions to evaluate contributions from different OCS sources in Venus' lower atmosphere.

Experimental Methods: The OCS formation reactions were studied at ambient atmospheric pressure in a gas-mixing vertical tube furnace. The same system was also used to investigate chemical weathering reactions on Venus [6,7]. Reacting gas mixtures at a flow rate of 150 cm^3/min (STP) were passed through the isothermal zone (~5 cm) at preset temperatures. Pyrite (FeS_2) was used in weathering reactions (reaction 2), as well as a source of S vapor (dominantly S_2) for reaction (1). The dependence of S_2 pressure (bar) on temperature is $\log_{10} P(S_2) = 16.20 - 15700/T$ [8]. The compositions of the starting gas mixtures and products were analyzed by an online gas chromatograph. A Matheson certified standard (98.3 ppmv OCS in He) was used to calibrate the OCS concentrations.

Results: There are several important observations: (1) Carbonyl sulfide (OCS) is formed by heating pyrite in CO-bearing gases at temperatures of 470° to 580°C in the laboratory, and the amount of OCS formed is directly proportional to the CO content in the gas mixture, as shown in Table 1. (2) Much smaller amounts of OCS are formed by heating pyrite in pure CO_2 at 538°–612°C, but the amounts of OCS formed are undetectable (<1 ppmv) at 471°C. (3) No detectable OCS was observed when heating a 0.50% CO–0.50% SO_2–CO_2 mixture at 470°C, although the predicted equilibrium OCS concentration is ~740 ppmv. (4) The pyrite decomposition rates at 470°C in CO/CO_2 and in inert gases (e.g., He, N_2) are the same. (5) No measurable amount of Fe_3O_4 was found in the product by XRD. (6) Pyrrhotite formed by pyrite decomposition in inert gases and CO_2 mixtures has the same composition at a given temperature.

Summary: Carbonyl sulfide formation from CO and S_2 is rapid, and is kinetically favored in the lower atmosphere of Venus. Carbonyl sulfide formation from reaction (3) between SO_2 and CO is much slower. Finally, reaction (2) apparently does not occur and pyrite thermally decomposes to pyrrhotite as shown by [6–8].

Acknowledgments: This work is supported by NASA grant NAGW-2867. We thank K. Lodders and M. Yu. Zolotov for helpful discussions.

References: [1] Fegley et al. (1997) *Icarus, 125*, 416. [2] Zolotov (1996) *Geochem. Intl., 33(10)*, 1551. [3] Von Zahn et al. (1983) in *Venus*, Univ. of Arizona, Tucson. [4] Prinn (1985) in *The Photochemistry of Atmospheres*, Academic, New York. [5] Fegley and Treiman (1992) in *Venus and Mars*, AGU Geophys. Mono. 66. [6] Fegley et al. (1995) *Icarus, 115*, 159. [7] Hong et al. (1996) *Eos Trans. AGU, 77*, F439. [8] Hong and Fegley (1997) *Planet. Space Sci.*, submitted.

MINERALOGY AND CHEMICAL COMPOSITIONS OF COLOMERA (IIE) SILICATE INCLUSIONS.

W. Hsu[1], H. Takeda[1,2], G. R. Huss[1], and G. J. Wasserburg[1], [1]Division of Geological and Planetary Sciences, 170-25, California Institute of Technology, Pasadena CA 91125, USA (whsu@gps.caltech.edu), [2]Chiba Institute of Technology, Narashino City, Chiba 275, Japan.

Irons of groups IAB and IIE contain silicate inclusions. In IAB irons, these inclusions are basically chondritic, but in IIE they vary from chondritic to highly differentiated [1,2]. In this work, we present detailed studies of mineralogy and trace-element geochemistry of eight silicate inclusions from Colomera with the goal of better understanding early planetary differ-

entiation and possible genetic relationships between iron and stony meteorites.

The typical major phases in Colomera silicates include an alkali-silica-rich glass (85% $Ab_{94}An_3Or_3$ plus 15% SiO_2) and orthopyroxene ($Wo_2En_{80}Fs_{18}$), which usually surrounds anhedral-to-euhedral Cr diopside ($Wo_{42}En_{46}Fs_{12}$). Minor phases include olivine ($Fo_{67}Fa_{33}$), Na feldspar, K feldspar, chlorapatite, whitlockite, chromite, rutile, troilite, and Fe metal. Apatite occurs either as minute inclusions (10–20 μm) in the glass or as large individual grains (400 μm). Whitlockite is found near the glass-metal interface.

Each inclusion has distinct mineralogy and modal abundances, and therefore is highly heterogeneous in terms of major-and trace-element concentrations. The figure shows two examples. Inclusion A contains 80% albitic glass and 20% whitlockite. The bulk pattern, calculated from modal abundances, is 10–30× CI and LREE enriched with a positive Yb anomaly. Inclusion B has 72% albitic glass, 20% diopside, 8% orthopyroxene, and no phosphates. The glass in this inclusion has negative Sm and Yb anomalies. The bulk REE pattern for the inclusion is HREE enriched with a negative Yb anomaly, with REEs at 1–6× CI.

Major-element compositions of Colomera inclusions are broadly consistent with an origin as low-temperature partial melting of chondritic material [3]. IIE silicates have O isotopic compositions similar to those of H chondrites [4]. The REE pattern for bulk Colomera silicates, as estimated from the range of patterns for individual inclusions, is essentially unfractionated, consistent with an origin from chondritic material. Colomera is a large (134 kg) iron mass with large silicate inclusions in its surface (including 11 cm sanidine crystal) and smaller globular-to-irregular alkali-silica-rich inclusions in its interior [5]. These observations suggest that Colomera originated when molten Fe was injected into chondritic material near the surface of an asteroid. Heat from molten Fe caused localized melting of the chondritic material and blobs of melt were incorporated into the Fe. Modal differences in the amount of phosphate, the main REE carrier, and other minerals between the sources of the melt blobs are reflected in the bulk compositions and REE abundances of the inclusions. The inclusions remained isolated from one another once they were incorporated into the metal melt. The Yb anomalies imply melting of silicates under highly reducing conditions similar to those for enstatite chondrites [6].

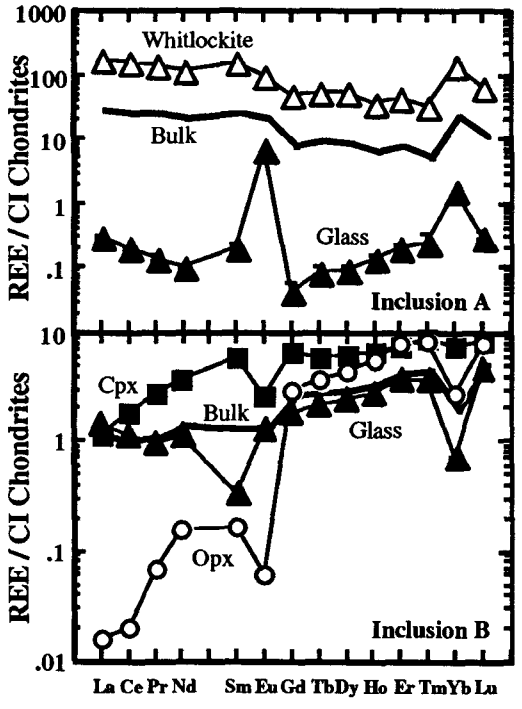

Fig. 1.

Acknowledgments: Supported by NASA grant NAGW-3297. Div. Contrib. 5822 (968).

References: [1] Bild R. W. (1977) *GCA, 41*, 1439–1456. [2] Bunch T. E. et al. (1970) *Contrib. Mineral. Petrol., 25*, 297–340. [3] Jurewicz A. J. G. (1993) *LPS XXIV*, 739–740. [4] Clayton et al. (1983) *EPSL, 65*, 229–232. [5] Wasserburg G. J. et al. (1968) *Science, 161*, 684–687. [6] Hsu W. and Crozaz G. (1995) *LPS XXVI*, 635–636.

NITROGEN AND ARGON IN INDIVIDUAL LUNAR SOIL GRAINS.

F. Humbert[1], B. Marty[1], and R. Wieler[2], [1]CRPG, 15 Rue Notre-Dame des Pauvres, F-54501 Vandoeuvre lès Nancy, France (franckh@crpg.cnrs-nancy.fr), [2]ETH Zürich, Isotope Geology, NO C61, CH-8092 Zürich, Switzerland.

The provenance of N in lunar soils and the variable $\delta^{15}N$ values [1] are controversial. Since N and solar noble-gas concentrations in bulk samples correlate, a solar-wind (SW) origin is often preferred [2,3]. Nitrogen/argon and N/Xe ratios are roughly 10× and 3× respectively, higher than values inferred for the Sun [4]. Some attributed this to loss of heavy solar noble gases Ar-Xe [3], whereas others proposed alternative N sources, like terrestrial or indigenous lunar N [5–7].

Argon:krypton:xenon ratios in single lunar grains are constant within a given sample [8], though different from solar values. This supports the conclusion, based on gas release by *in vacuo* etching [9], that the samples conserve the relative abundances of Ar-Xe in the SW. Xenon in the SW is enhanced ~4× relative to Ar, similar to elements with a low first ionization potential (FIP). If N is mostly solar, then Ar, Kr, and Xe would all have to become depleted on the Moon about 10× relative to N (N and Ar are high-FIP elements). We therefore determined $^{14}N/^{36}Ar$ in individual grains of soil 71501 by laser heating.

The N_2 blanks are $(2–4.5) \times 10^{-12}$ moles, but constant within $\sim 0.5 \times 10^{-12}$ moles during a day. The N_2 amounts range between $(7–25) \times 10^{-12}$ moles in 500-μm grains and around 3×10^{-12} moles in 200-μm grains. Errors of $^{14}N/^{36}Ar$ ratios are <20% for most grains. Cosmogenic N so far prevents determination of $\delta^{15}N$ of trapped N, but stepwise heating with further reduced blanks is planned. Atmospheric ^{36}Ar and cosmogenic ^{14}N and ^{36}Ar are negligible.

Ignoring one apparently N-free grain, $^{14}N/^{36}Ar$ ratios vary between 41 and 970 (Fig. 1). The lowest value is close to the solar ratio of ~37 [4]. The weighted mean is ~200, lower than values of 270–340 in multigrain samples [10]. Nitrogen is not lost in our system, however, at the level relevant here (except perhaps for the one aberrant grain).

The ~25-fold variation of N/Ar strikingly contrasts with the constant Ar:Kr:Xe ratios in this soil [8]. If the N/Ar scatter were due to a highly variable Ar loss, we would not expect the observed uniform noble-gas elemental ratios. This suggests that in most grains an unknown N component

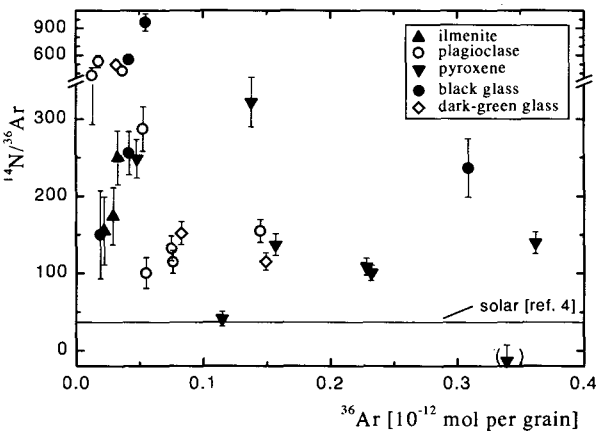

Fig. 1.